Cloud Publications
International Journal of Advanced Remote Sensing and GIS
2019, Volume 8, Issue 1, pp. 2919-2932
ISSN 2320 – 0243, Crossref: 10.23953/cloud.ijarsg.400

Research Article

Estimation of Air Pollution Using Multi-Temporal Remote Sensing Technique for Dehradun District, Uttarakhand

Jyotsana Joshi, Kishor Chandra Kandpal, Neelam Rawat

Uttarakhand Space Application Centre, Dehradun, Uttarakhand, India

Correspondence should be addressed to *kandpalkishor128@gmail.com*

Publication Date: 16 January 2019

DOI: https://doi.org/10.23953/cloud.ijarsg.400

Abstract Air pollution is a major problem of many countries around the world. The main source of the air pollution due to growing urbanization, growth of the industry, vehicles etc. In this research produce an empirical model using Landsat 8 satellite data and ground PM 10 measurement for determination of particulate matter (PM 10) concentration in the atmosphere over Dehradun city, the capital of Uttarakhand . The research focus on air pollution determination using atmospheric reflectance (DOS method) and correlate to PM 10 ground measurement**.** The outcomes of this research showed that visible bands of Landsat 8 OLI were capable of calculating PM10 concentration to an acceptable level of accuracy.
Keywords *Air Pollution; AOT; DOS; PM10; Reflectance*

1. Introduction

Air pollution is a universally major issue to human being. It causes various health problems and effects on natural environment i.e. increase the level of temperature. Major industrialization, is the main source of air pollution and other cause of dispersion of air pollution, including emission from vehicle, weather condition, humidity, presence of building and thermal power plant. Air pollution consequently shows high spatial variability, even at short distances (Wijeratne et al., 2006). According to 2014 report of World Health Organization (WHO), 92% of the world population was living in places where WHO air quality guideline standards were not met. Outdoor air pollution in both cities and rural areas was estimated to have caused 3 million deaths worldwide in 2012.

Particulate matter (PM10) pollution consists of very small liquid and solid particles which diameter is less than 10 micrometer or less floating in the air. PM10 is a major component of air pollution that threatens both our health and our environment. (Masitah et al., 2007). Particles in this size range make up a large proportion of dust that can be drawn deep into the lungs. Larger particles tend to be trapped in the nose, mouth or throat. The study of particulate matter (PM) as air pollutant is important because of its effects on human health, atmospheric visibility, climate change, etc. (Leli et al., 2008). So mapping of air quality is important for the assessment of annual, seasonal changes and other environmental climate changes. Traditionally, two general approaches to mapping air pollution can be identified: spatial interpolation and air dispersion modeling (Elliott et al., 1996). The former approaches estimate the value of pollution concentration at un-sampled locations in an area of interest by

interpolating the measurements from the sampled stations (Masitah et al., 2007). Most of the air quality data that currently used are interpolated from the data collected from a limited number of measuring stations located mainly in cities or estimated by the numerical air dispersion models (Retalis et al., 2010).

Air pollutants can be measured from ground base stations with many different types of instruments. But these instruments are quite expensive and limited by the number of air pollutant station in each area. The limited number of the air pollutant stations and improper distributed not allowed a proper mapping of the air pollutants. Ground instruments are impractical if measurements are to be made over large areas or for continuous monitoring. So, they cannot provide a detail spatial distribution of the air pollutant over large cities.

This study focuses on the mapping of dispersion of air pollution using remote sensing techniques and ground station data. The basic method is a radiometric comparison of a satellite image recorded under polluted conditions, with a reference image acquired under less polluted condition. Ground station data were used to select a less polluted reference image. In remote sensing, different algorithms are used to estimate particulate matter (PM10), depending on the sensor and the spectral band (Sifakis and Deschamps, 1992; Sifakis et al., 1998; Retalis et al., 1999; Wald and Baleynaud, 1999; Ung et al., 2001). The relation between ground observations and estimates of aerosol optical thickness is described with linear regression providing the spatial distribution of air pollution. Therefore, in this study presented the potentiality of retrieving concentrations of particulate matter with diameters less than ten micrometer (PM10) in the atmosphere using the Landsat 8 satellite images over Dehradun. The main aim of the study is to finding a suitable empirical equation for the estimation of particulate matter using remote sensing technology and ground data.

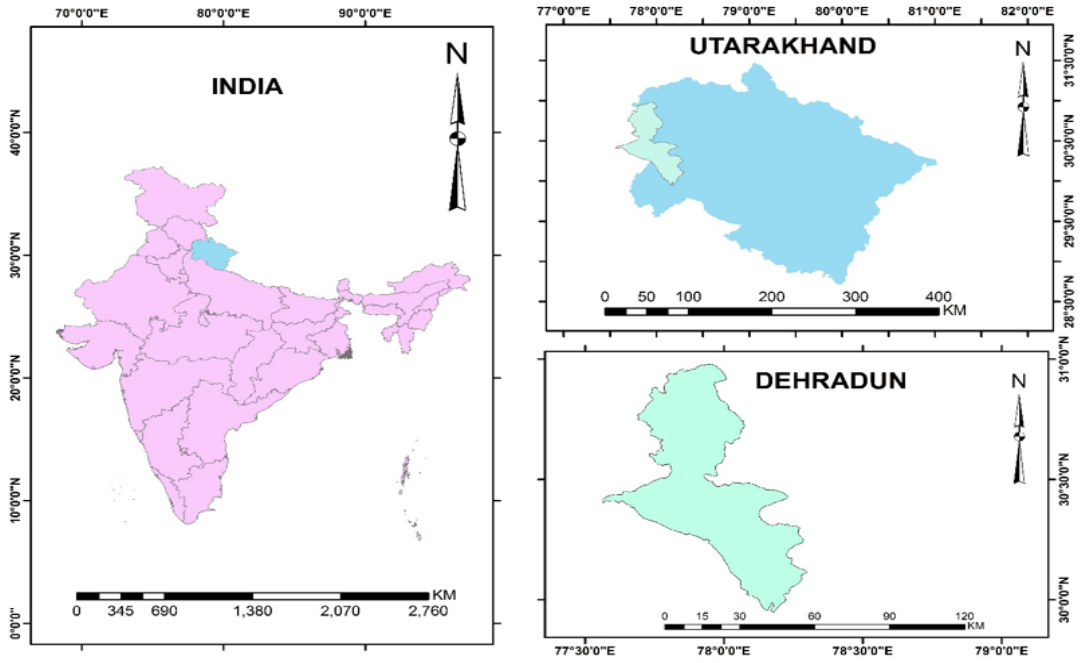

Figure 1: *Location map of study area*

Study Area

Dehradun district covers an area of 3,088 km^2 (1,192 sq mi). Geographical extension of Dehradun is between 78°00'E to 78°15'E longitudes and 30°15'north to 30°25'N latitudes. Dehradun is located in a synclinal valley within the Siwalik formation. Rocks under Siwalik formation were thrusted over the sediments of Indo-Gangetic Plain along the Himalayan Frontal Fault (Ori and Friend, 1984; Gupta, 1997). On the east, the Dehradun town is surrounded by the Song River, the Tons River on the west, the Himalaya ranges on the north and the south by Sal forests.

2. Materials and Methodology

The methodology process generally was divided into the four steps: data acquisition, pre-processing, data processing and validation of results. Arc GIS 10.4, ERDAS IMAGINE 14 and SPSS are used for the study.

Pre-processing

In the first step, the raw digital number (DN) values of Landsat imagery have been converted to radiance value. In the second step, the radiance value are converted to top of atmospheric reflectance (TOA).

Conversion to TOA Radiance

OLI and TIRS band data can be converted to TOA spectral radiance using the radiance rescaling factors provided in the metadata file:

$$L\lambda = ML*Qcal + AL \ldots (1)$$

Where:

Lλ = TOA spectral radiance [Watts/(m2 * srad * μm)]
ML = Band-specific multiplicative rescaling factor from the metadata
(RADIANCE_MULT_BAND_x, where x is the band number)
AL = Band-specific additive rescaling factor from the metadata
(RADIANCE_ADD_BAND_x, where x is the band number)
Qcal = Quantized and calibrated standard product pixel values (DN)

Conversion to TOA Reflectance

OLI band data can also be converted to TOA planetary reflectance using reflectance rescaling coefficients provided in the product metadata file (MTL file). The following equation is used to convert DN values to TOA reflectance for OLI data as follows:

$$\rho\lambda' = M\rho*Qcal + Ap \ldots (2)$$

Where:

ρλ' = TOA planetary reflectance, without correction for solar angle. Note that ρλ' does not contain a correction for the sun angle.

Mρ = Band-specific multiplicative rescaling factor from the metadata (REFLECTANCE_MULT_BAND_x, where x is the band number)
Aρ = Band-specific additive rescaling factor from the metadata (REFLECTANCE_ADD_BAND_x, where x is the band number)
Qcal = Quantized and calibrated standard product pixel values (DN)
TOA reflectance with a correction for the sun angle is then:

$$\rho\lambda = \rho\lambda'/\sin(\theta) \quad \ldots (3)$$

Where:

ρλ = TOA Planetary Reflectance (Unit less)
θ = Solar Elevation Angle (from the metadata, or calculated)

Atmospheric Correction

It is worth pointing out that Landsat 8 images are provided with band-specific rescaling factors that allow for the direct conversion from DN to TOA reflectance. However, the effects of the atmosphere (i.e. a disturbance on the reflectance that varies with the wavelength) should be considered in order to measure the reflectance at the ground. As described by Moran et al. (1992), the land surface reflectance (ρ) is:

$$\rho = \frac{\pi * (L\lambda - Lp) * d^2}{Tv * \{(ESUN\lambda * cos\theta * TZ)} \quad \ldots (4)$$

Where:

LP = path radiance
TV = atmospheric transmittance in the viewing direction
TZ = atmospheric transmittance in the illumination direction
Edown = downwelling diffuse irradiance
ESUNλ = mean solar exo-atmospheric irradiances
d = earth_sun distance (provided with Landsat 8 metadata)

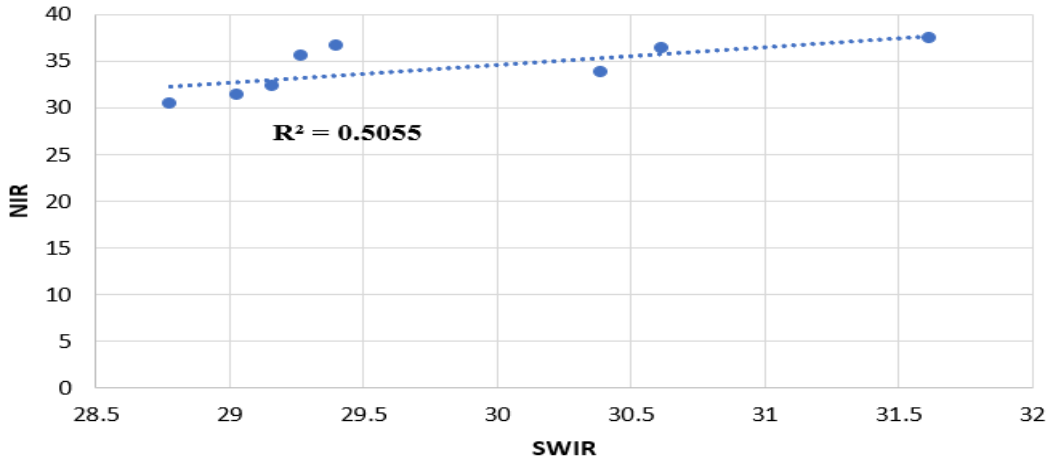

Figure 2: *Correlation between SWIR and NIR for DOS method*

Path Radiance (Using Dark object subtraction Method) DOS

This approach indicates lower Lp with increasing wavelength and negligible Lp in SWIR band. Correlation with SWIR band with NIR, Red, Green and Blue individually, and found that correlation as high as 0.50 for NIR band, 0.16 for Red band and 0.12 for Blue band. Then subtract minimum radiance value of NIR band from each visible band.

And the resulting land surface reflectance is given by:

$$\rho = \frac{\pi * (L\lambda - Lp) * d^2}{ESUN\lambda * \cos\theta sz} \quad \text{... (5)}$$

Atmospheric Reflectance

Atmospheric reflectance is calculated as:

AR = TOA – Surface Reflectance … (6)

Particulate matter (PM), also known as particle pollution, is a complex mixture of extremely small particles and liquid droplets that get into the air. Once inhaled, these particles can affect the heart and lungs and cause serious health effects.

Here in this Study PM10 is estimated by Multiple Regression Analysis, the result was extended to a three and four-band algorithm as:

A = e + e R1 + e R2 + e R3+ e R … (7)

Where:

A = Particle concentration (PM10)
Ratmi = Atmospheric reflectance, i = 0, 1 and 3 are the band number
e = algorithm coefficients

Regression Analysis and Mapping

Using linear regression, we established relations between processed image outputs (PM10) and ground data of PM10.

Linear Regression

Y = a + bX … (8)

Multiple Regression

Y = a + b1X1 + b2X2 + b3X3 +b3X4 … (9)

Where:

Y = the variable that you are trying to predict (dependent variable)
X = the variable that you are using to predict Y (independent variable)

a = the intercept
b = the slope

3. Results and Discussion

The digital numbers of the four visible bands namely blue, green, red and NIR of Landsat 8 OLI were extracted corresponding to the locations of ground PM10 measurements over Dehradun district. The Landsat visible band converted into Radiance, TOA and then surface reflectance using DOS method. The atmospheric reflectance calculated from the surface reflectance subtracted from TOA reflectance. The scatter plot of visible bands of atmospheric reflectance correlate to PM 10 ground measurements is shown in following figures.

Table 1: *Calculated PM10 Concentration from Satellite Image Data and PM10 Ground Measurement at Different Location of Dehradun District (2013)*

Ground station	pm10 concentration estimated from Imagery (µg/m³)	Monthly average pm10 concentration measured at ground station (µg/m³)
Clock tower	154.12	159
Raipur road	163.63	166
ISBT	183.74	182
Rishikesh	121.79	123

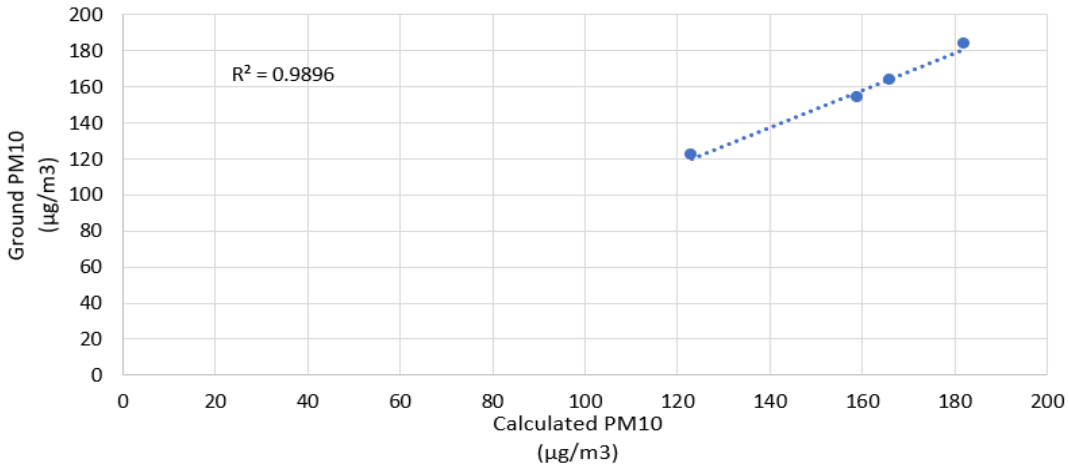

Figure 3: *Regression analysis between calculated PM10 and Ground PM10 (2013)*

Table 2: *Calculated PM10 concentration from satellite image data and PM10 ground measurement at different location of Dehradun District (2015)*

Ground station	PM10 concentration estimated from Imagery (µg/m3)	Monthly Average pm10 concentration measured at ground station (µg/m3)
Clock Tower	191.75	173
Raipur Road	188.67	159
ISBT	201.44	226
Rishikesh	174.32	156

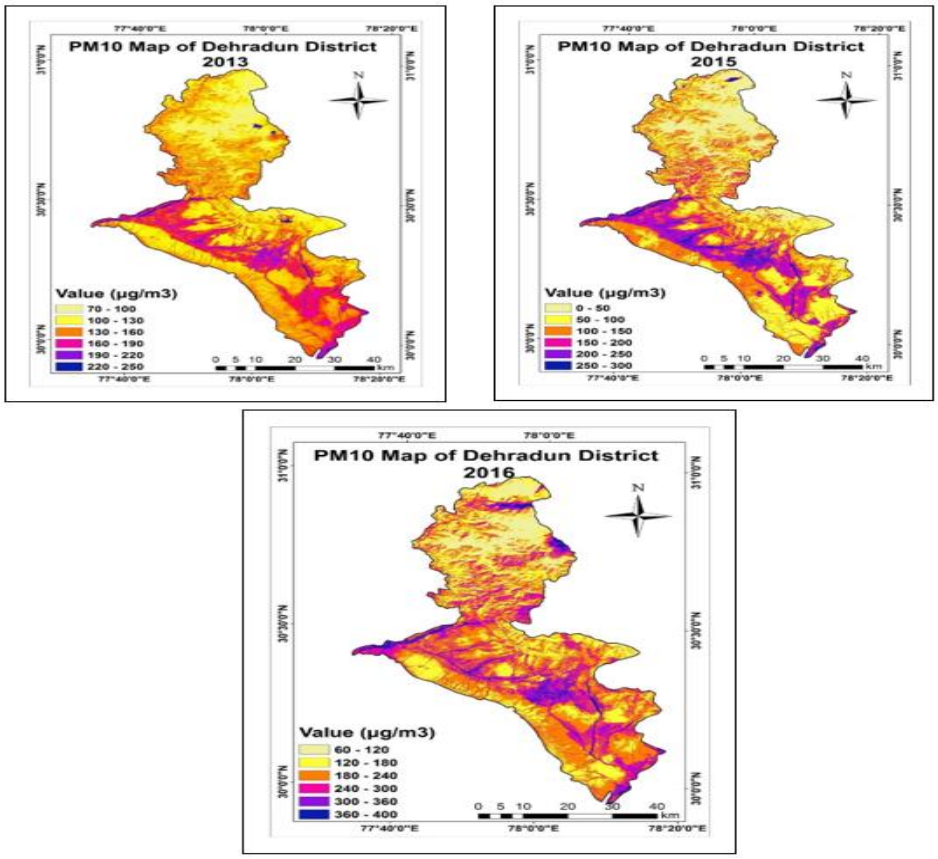

Figure 4: *PM10 Concentration Over Dehradun District (2013, 2015, 2016)*

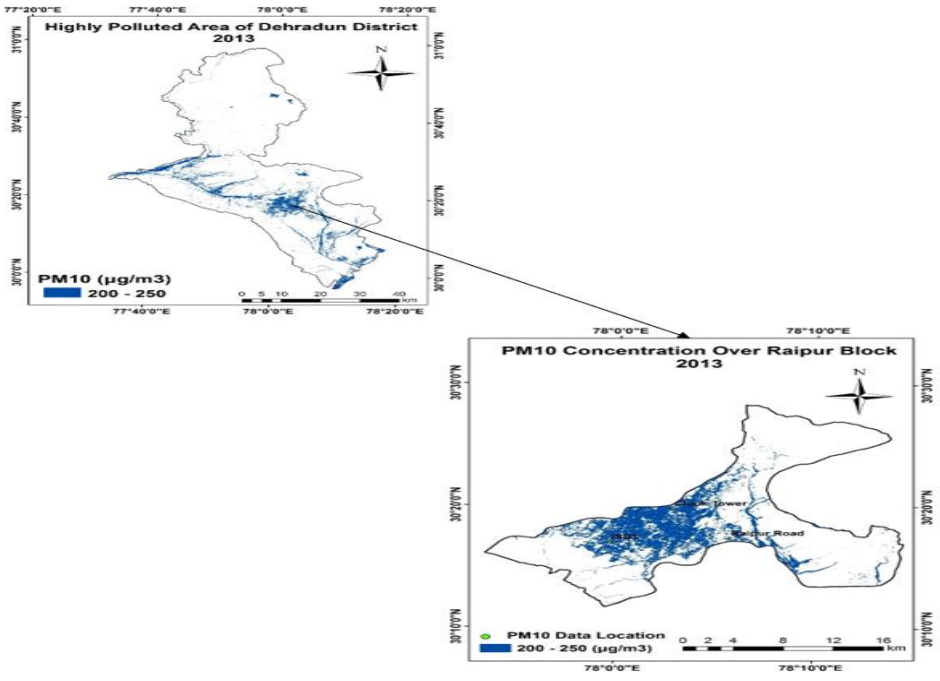

Figure 5: *Highly polluted area of Dehradun City (2013)*

In the Dehradun district, there are four PM 10 ground station i.e. Clock tower, ISBT, Risikesh and Raipur Road. The maximum concentration of calculated PM 10 was 201.44 µg/m³ at ISBT in Dehradun as calculated for May, 2013. It is observed that the minimum concentration of calculated PM 10 was 174.32 µg/m³ at Risikesh (Table 2). From Table 2, it can be observed that the concentration of PM 10 increased from 201.44 µg/m³ to 375.39 µg/m³ for 2016 and shifted from ISBT to Raipur road due to the urbanization at Raipur Road. The minimum concentration of PM 10 increased from 174.32 µg/m³ to 190.01 µg/m³ for 2016 at Rishikesh

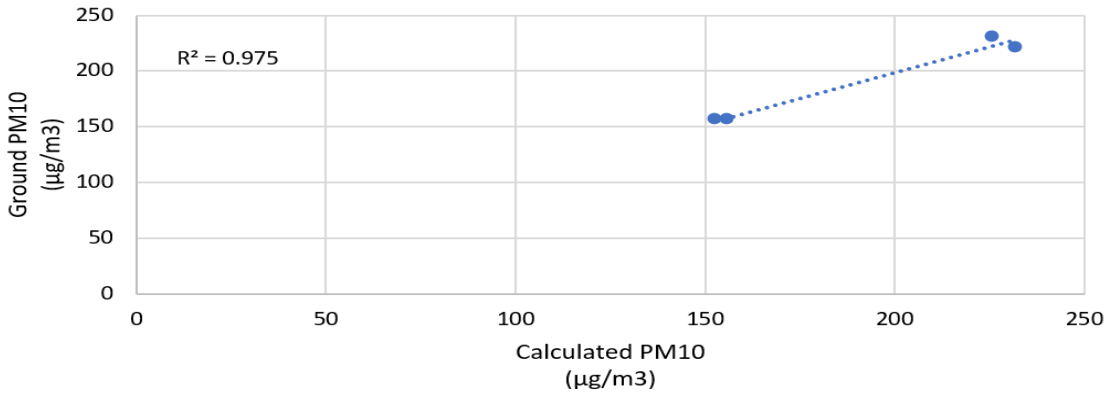

Figure 6: *Regression analysis between calculated PM10 and Ground PM10 (2015)*

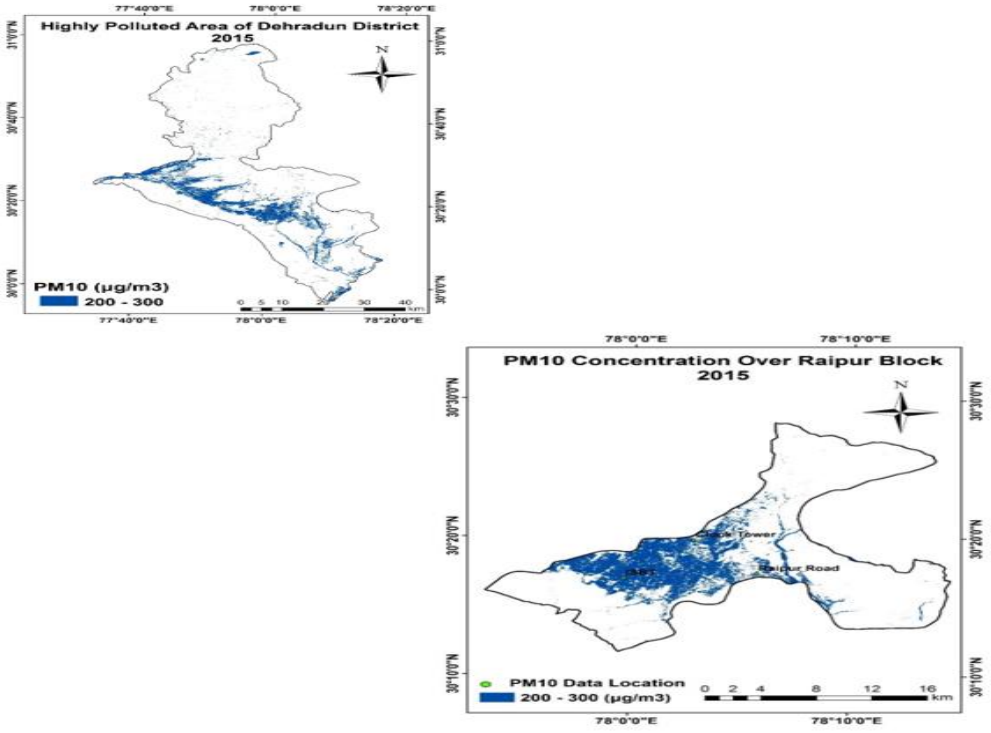

Figure 7: *Highly polluted area of Dehradun City (2015)*

Table 3: *Calculated PM10 concentration from satellite image data and PM10 ground measurement at different location of Dehradun District (2016)*

Ground station	pm10 concentration estimated from imagery (µg/m3)	Monthly average pm10 concentration measured at ground station (µg/m3)
Clock tower	206.48	209.79
Raipur road	375.39	377.76
ISBT	312.29	316.04
Rishikesh	190.01	197.13

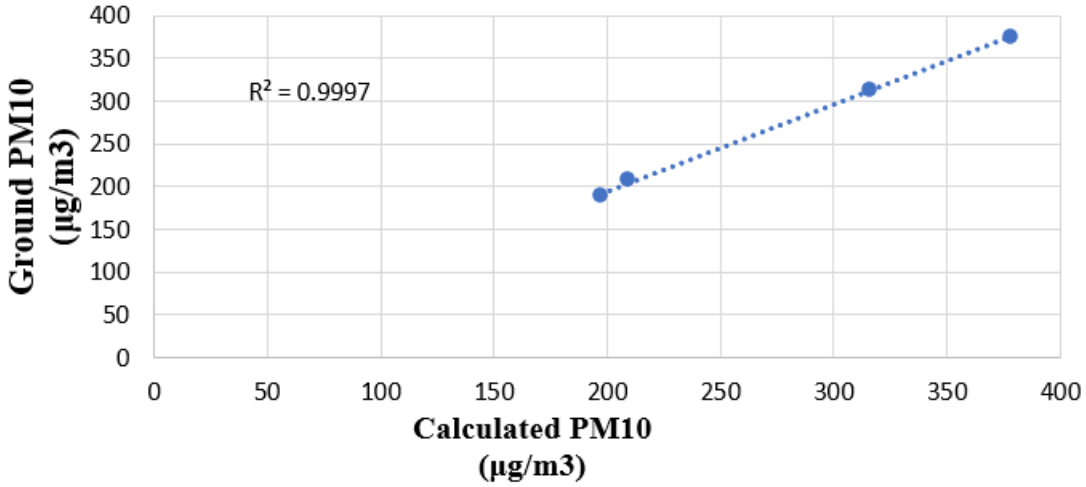

Figure 8: *Regression analysis between calculated PM10 and Ground PM10 (2016)*

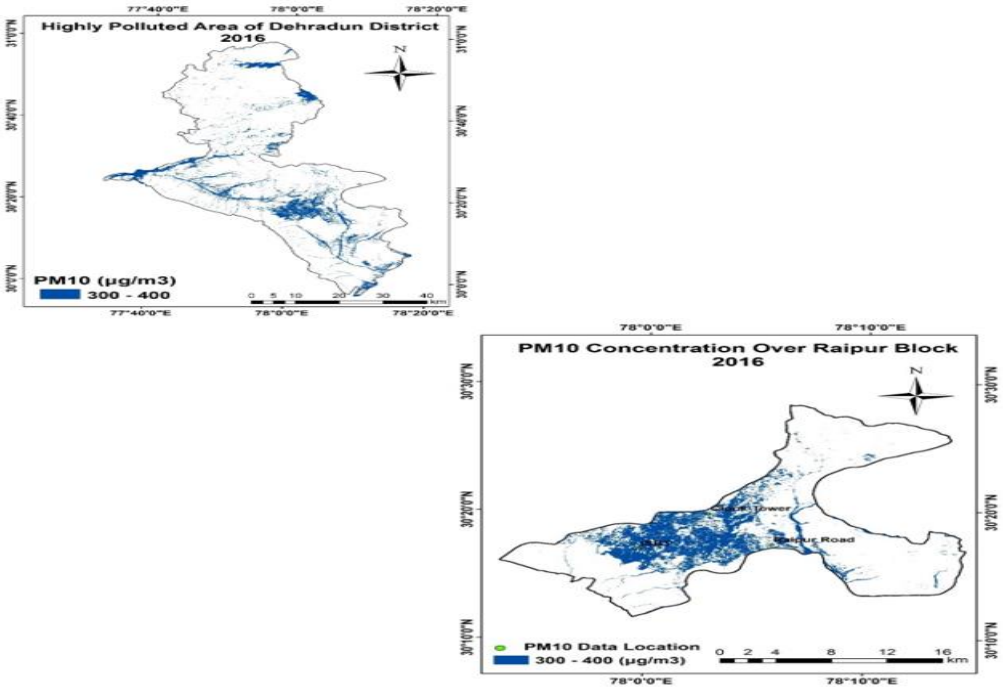

Figure 9: *Highly polluted area of Dehradun City (2016)*

The present paper highlighted the assessment of spatio-temporal pattern of PM 10 concentration during 2013, 2015 and 2016 over Dehradun -capital of the Uttarakhand and PM 10 changes during 3 years. The current study utilized Landsat data from 2013 to 2016 and validate with PM 10 ground station measurements. The atmospheric reflectance for blue, green and red bands were determined using equation (6), as shows in Figure (10-12). For the study, atmospheric reflectance values correlate with different bands, which is adjusted at the ground measurements due to lowest RMSE and highest R.

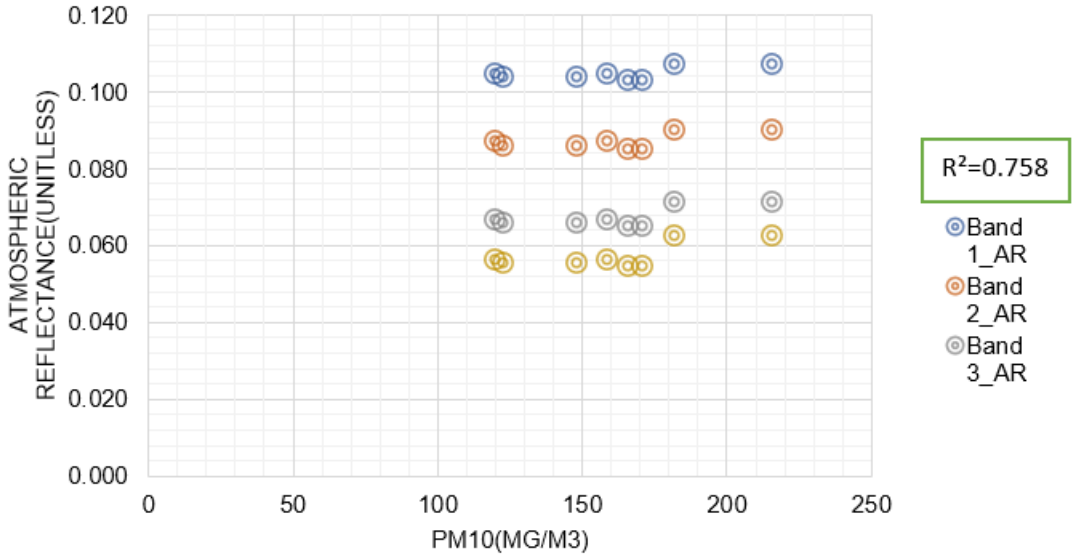

Figure 10: *Multiple regression between AR and PM10 estimated from ground (2013)*

Linear regression analysis is carried out to find the relationship between Atmospheric reflectance and ground PM 10 concentration. In the first part of analysis atmospheric reflectance of blue, green, red and NIR and ground PM10 concentration correlated separately. These resultant value of R^2 is less than 0.4. Therefore, Multiple linear regression analysis was used to develop a model for PM10 estimation, and the value of R^2=0.758 for 2013, R^2=0.531 for 2015 and R^2=0.841 for 2016.

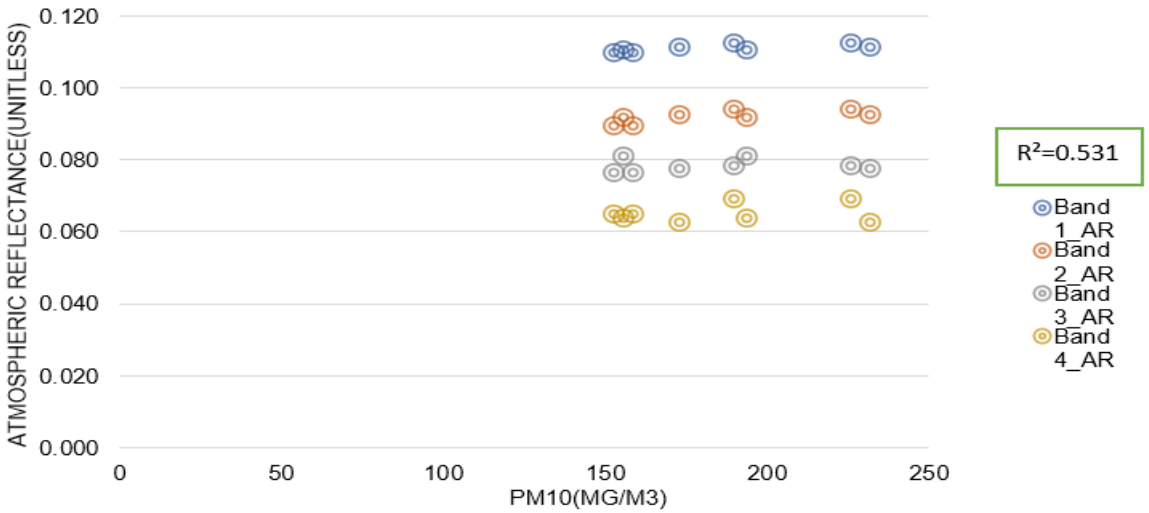

Figure 11: *Multiple regression between AR and PM10 estimated from ground (2015)*

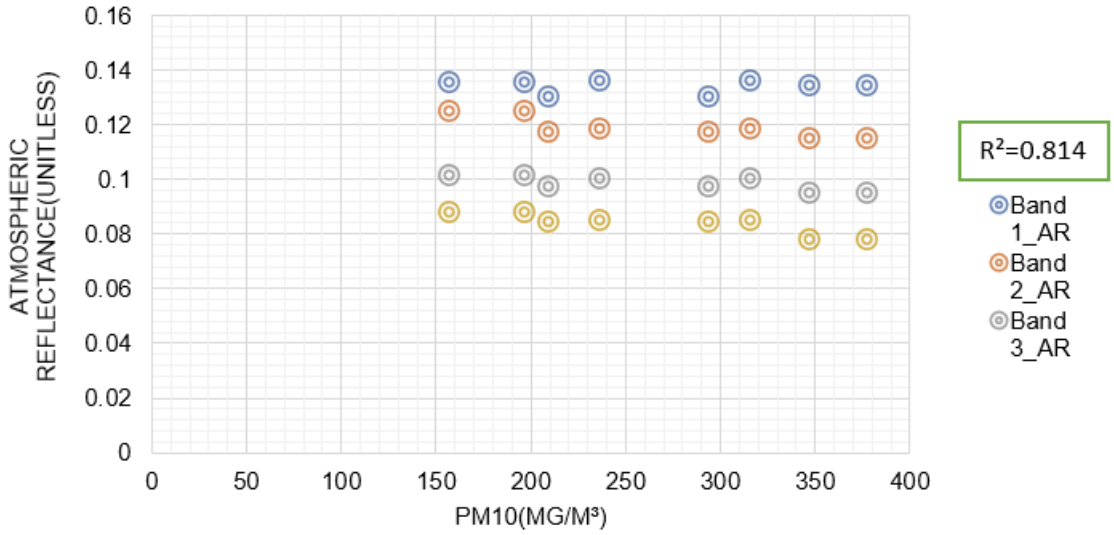

Figure 12: *Multiple regression between AR and PM10 estimated from ground (2016)*

Table 4: *Regression results (R) using different forms of algorithms. Calculated PM10 by algorithms, b1, b2, b3 and b4 are the reflectance values for band1, band2, band3 and band4 of Landsat 8 OLI*

S. No.	Algorithm	R^2
1.	PM10 = 0.00004b1 + 0.0986	0.02545
2.	PM10 = 0.00005b2 + 0.0787	0.366
3.	PM10 = 0.00007b3 + 0.0563	0.3875
4.	PM10 = 0.00009b4 + 0.0431	0.4014
5.	PM10 = -1069.36 + 5686.114b1 + 11564.33b2 – 3091.88b3 – 3090.33b4	0.9868
6.	PM10 = 0.00002b1 + 0.1063	0.7125
7.	PM10 = 0.00004b2 + 0.085	0.7133
8.	PM10 = -0.000006b3 + 0.063	0.018
9.	PM10 = 0.00001b4 + 0.0623	0.0461
10.	PM10 = 59.852 – 16563.4b1 + 25293.48b2 – 4615.48b3	0.5316
11.	PM10 = 0.00001b1 + 01305	0.1503
12.	PM10 = -0.00003b2 + 0.1284	0.4858
13.	PM10 = -0.00002b3 + 0.1031	0.3037
14.	PM10 = -0.00004b4 + 0.0940	0.06609
15.	PM10 = -2914.44 + 5152.015b1 + 7675.03b2 + 19199.64b3 – 3666.89b4	0.9615

A linear regression is used to create PM 10 algorithm based on highest value of R where the R=, for 2013, R= for 2015, and R= for 2016. The PM 10 algorithm is as below equation (5) for 2013, equation (10) for 2015 and equation (15) for 2016.

PM10 = -1069.36 + 5686.114b1 + 11564.33b2 – 3091.88b3 – 3090.33b4 (5)
PM10 = 59.852 – 16563.4b1 + 25293.48b2 – 4615.48b3s (10)
PM10 = -2914.44 + 5152.015b1 + 7675.03b2 + 19199.64b3 – 3666.89b4 (15)

Where PM 10 is the PM 10 concentration (γ g/m³), Ratm(γ 1), Ratm(γ 2), R(γ and R(γ are atmospheric reflectance of visible band.

Temporal Variation of PM10 Concentration

Below the graph shows the average monthly concentration for PM10, during the year 2013, the average PM10 recorded are 160.16 µg/m3, during the year 2015, the average PM10 recorded are 185.37 µg/m3 and in the year of 2016, the average PM10 recorded are 266.95 µg/m3 the result show that the average monthly PM10 concentration are increased during the year 2013, 2015, 2016.

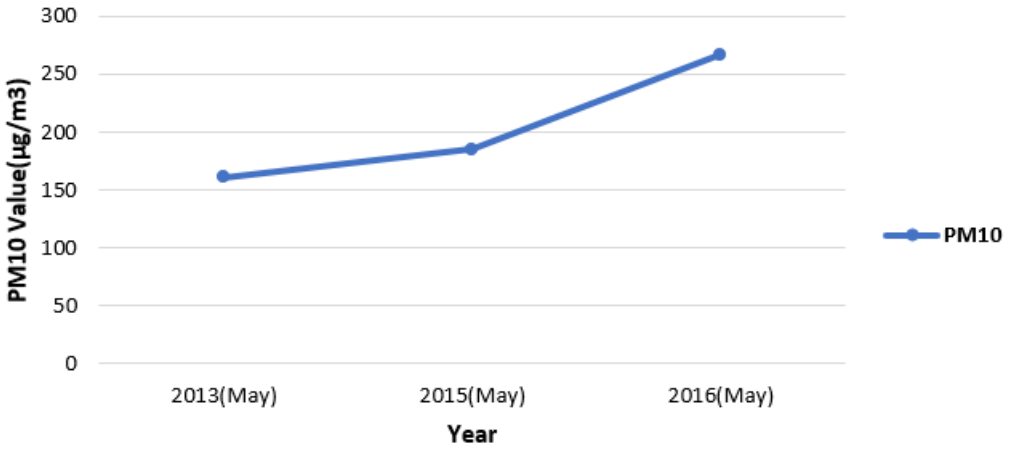

Figure 13: *Multi temporal graph of PM10*

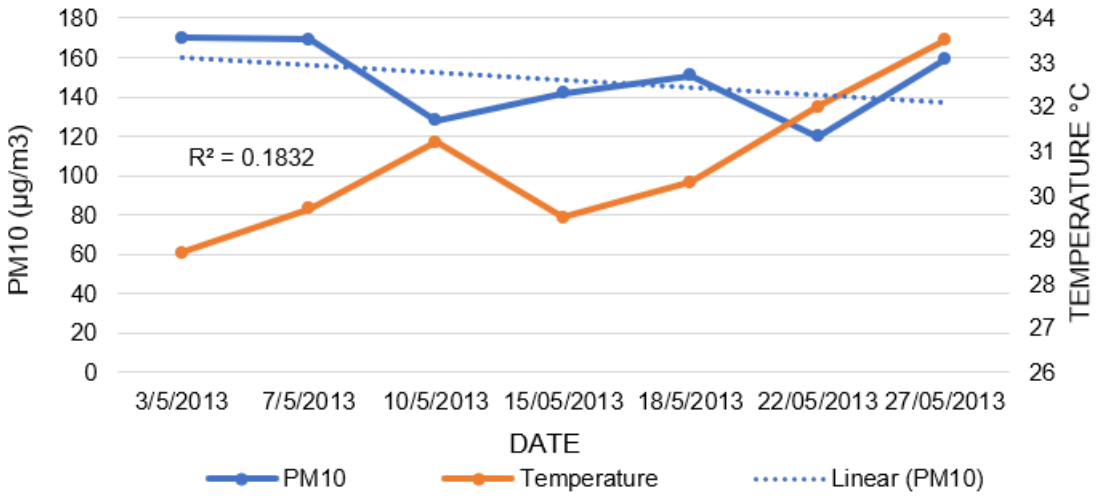

Figure 14: *The relationship graph between air temperature and PM10 (2013)*

The Relationship between Concentrations of Particulate Matter and Air Temperature

From the following figure, it can be observed that concentrations of PM10 had an obviously negative correlation with air temperature. As air temperature increased, concentration of particulate matter was significantly decreased. Because intense radiation heats city underlying surface. The lower atmosphere is not very stable and turbulent strengthens, which is advantages to the diffusion of

pollutants. Therefore, the probability of atmospheric pollution decreased with the increased of the air temperature in summer. While the temperature of surface low, the situation is contrary(Tian et. al 2014)

4. Conclusion

Remote Sensing and GIS based technique was used to estimate air pollution and identify the most polluted area of Dehradun district. The calculation of PM10 concentration using the visible bands reflectance value of Landat 8 imagery. The result show that the urban area of Dehradun district more polluted. This study also prove air pollution can be mapped using satellite data to provide a large coverage.

- The primary assumption about air pollutant particle, the solar irradiance did not reach earth surface, so the solar irradiance interact to atmospheric pollutants. Thus the atmospheric reflectance directly correlate to ground PM 10 measurements.
- In this present study, developed an algorithm to estimate the PM10 concentration over Dehradun District based on Landsat image data and ground monitoring stations data. Three years data has been used to validate the algorithm.
- The present study suggests that we can monitor PM10 concentration on large coverage, if we have selected or less ground PM10 stations.
- The result show that the average monthly PM10 concentration is increased during the year 2013, 2015, 2016.
- The major urban area of Dehradun district is doon valley and the highest PM10 concentration is found with in doon valley and is constantly increasing over the valley.

References

Bozyazi, E.G. 1998. *Analysis and mapping of air pollution: a GIS approach: A case study of Istanbul, Turkey*. MSc thesis, International Institute for Aerospace Survey and Earth Sciences (ITC), Enschede, The Netherlands.

Chakraborty, J., Schweitzer, L.A. and Forkenbrock, D.J. 1999. Using GIS to assess the environmental justice consequences of transportation system changes. *Transactions in GIS*, 3(3), pp.239–258.

Cheng, S. and Lam, K.C. 1997. *Climatic Impact on air pollution concentrations in Hong Kong. Department of Geography*. Occasional paper, The Chinese University of Hong Kong, Hong Kong.

Duk-Dong, L. and Dae-Sik, L. 2001. Environmental gas sensors. *IEEE Sensors Journal*, 1(3).

El Desouky, H.J., Moussa, K.F. and Hassona, H.H. 1998. Impact of automobile exhaust on roadside-soils and plants in Sharkiya Governorate. *Egyptian Journal of Soil Science*, 38(1-4), pp.137-151.

Hadjimitsis, D.G., Nisantzi, A., Themistocleous, K., Matsas, A. and Trigkas, V.P. 2010. *Satellite remote sensing, GIS and sun-photometers for monitoring PM10 in Cyprus: issues on public health*. Proceedings of SPIE - The International Society for Optical Engineering, 7826, 78262C.

Hadjimitsis, D.G., Clayton C.R.I. and Hope, V.S. 2004. An assessment of the effectiveness of atmospheric correction algorithms through the remote sensing of some reservoirs. *International Journal of Remote Sensing*, 25(18), pp.3651-3674.

van de, K.J. 2006. Statistical air quality mapping. Ph.d. thesis, Wageningen University, Wageningen, The Netherlands.

Lee, H.J., Liu, Y., Coull, B.A., Schwartz, J. and Koutrakis, P. 2011. A novel calibration approach of MODIS AOD data to predict PM2.5 concentrations. *Atmos. Chem. Phys.*, 11, pp.7991-8002.

McCubbin, D.R. and Delucchi, M.A. 1999. The health costs of motor vehicle related air pollution. *Journal of Transport Economics and Policy*, 33(3), pp.253-286.

Mishra. R.K., Pandey. J., Chaudhary. S.K., Khalkho A. and Singh. V.K. 2013. Estimation of air pollution concentration over Jharia coal field. *International Journal of Geomatics and Geosciences*, 4(1).

Nadzri, O., Mohd, Z.M.J. and Lim, H.S. 2010. Estimating particulate matter concentration over arid region using satellite remote sensing: a case study in Makkah, Saudi Arabia. Modern Applied Science, 4, pp.131-142.

Nhu Hung, N. and Van Anh, T. 2014. Estimation of Pm10 From AOT of satellite Landsat 8 image over Hanoi city. *International Symposium on Geoinformatics for Spatial Infrastructure Development in Earth and Allied Sciences*.

Nisantzi A., Hadjimitsis D.G. and Aexakis, D. 2011. *Estimating the relationship between aerosol optical thickness and PM10 using lidar and meteorological data in Limassol, Cyprus*. SPIE Remote Sensing.

Retalis, A., Hadjimitsis, D.G., Chrysoulakis, N., Michaelides, S. and Clayton, C.R.I. 2010. Comparison between visibility measurements obtained from satellites and ground. *Natural Hazards and Earth System Sciences Journal*, 10(3) pp.421-428.

Hameed Saleh, S.A. and Ghada H. 2014. Estimation of PM10 concentration using ground measurements landsat 8 OLI satellite image. *Geophysics & Remote Sensing*, 3, p.2.

Zhang Jin, T., Pouyat, R. and Zhang, J.T. 2000. Effects of urbanization on the concentrations of heavy metals in deciduous forest floor in a case study of New York City. *Scientia Silvae Sinicae*, 36(4), pp.42-45.